



Integration of support vector regression and grey wolf optimization for estimating the ultimate bearing capacity in concrete-filled steel tube columns

Ngoc-Tri Ngo¹ · Hoang An Le² · Thi-Phuong-Trang Pham³

Received: 10 August 2020 / Accepted: 11 December 2020 / Published online: 3 January 2021
© The Author(s), under exclusive licence to Springer-Verlag London Ltd. part of Springer Nature 2021

Abstract

Concrete-filled steel tube (CFST) columns are widely used in the construction industry. Prediction of the ultimate bearing capacity of CFST columns is complicated because it is influenced nonlinearly by many factors such as steel tube length, steel tube thickness, ratio length and column diameter, and concrete compressive strength. This study proposes an artificial intelligence (AI) model to predict the ultimate bearing capacity of CFST columns. The AI model was developed based on support vector regression (SVR) and grey wolf optimization (GWO). The GWO optimized the SVR configuration that produces highly accurate prediction results. A large experimental dataset with normal, high, and ultimate strength concretes was used to validate the model's effectiveness through the learning and test phases. A k -fold cross-validation method was adopted to ensure the generalizability. The column diameter (D), thickness of steel tube (t), yield stress of steel, compressive strength of concrete, column length, D/t ratio were used as inputs for the model. Results show that the proposed SVR-GWO model was more effective than the compared models and empirical methods in the bearing capacity prediction of CFST columns. The SVR-GWO yielded the outstanding performance in which the accuracy improvements by the proposed model were ranged from 10.3 to 87.9% in the mean absolute percentage error and from 15.4 to 74.2% in the mean absolute error compared to baseline models and empirical methods. As contributions, the study suggested an AI-based tool for estimating the ultimate bearing capacity of CFST columns in structural design.

Keywords Concrete-filled steel tube column · Artificial intelligence · Regression · Optimization

List of symbols

CFST Concrete-filled steel tube
RC Reinforced concrete
NSC Normal strength concrete

HSC High-strength concrete
UHSC Ultra-high-strength concrete
UBC Ultimate bearing capacity
 L Steel tube length
 t Steel tube thickness
 D Column diameter
 L/D Ratio length and diameter of CFST columns
EC4 Eurocode 4
AISC American standards
AI Artificial intelligence
MARS Multivariate adaptive regression splines
M5Tree M5 model tree
SVR Support vector regression
GEP Gene expression programming
ANNs Artificial neural networks
PSO Particle swarm optimization
GA Genetic algorithms
 e/D Ratio of eccentricity to diameter
 $\bar{\lambda}$ Relative slenderness

✉ Ngoc-Tri Ngo
trinn@dut.udn.vn

Hoang An Le
lhan@ntt.edu.vn

Thi-Phuong-Trang Pham
ptptrang@ute.udn.vn

¹ Faculty of Project Management, The University of Danang, University of Science and Technology, 54 Nguyen Luong Bang, Danang, Vietnam

² NTT Hi-Tech Institute, Nguyen Tat Thanh University, Ho Chi Minh City, Vietnam

³ Department of Civil Engineering, The University of Danang, University of Technology and Education, 48 Cao Thang Street, Da Nang City, Vietnam

$N_{pl,Rd}$	Plastic cross-sectional resistance under compression
η_c	Confinement coefficient of concretes
η_a	Confinement coefficient of steel tubes
A_s	Section areas of the steel
A_c	Section areas of concrete
f_y	Yield strength of the steel
f_c	Unconfined concrete compressive strength
N_{cr}	Elastic critical normal force for the relevant buckling mode
$(EI)_{eff}$	Effective flexural stiffness
K_e	Correction factor
E_{c2}	Concrete elastic modulus
I_s	Moment of inertia of steel tube
I_c	Moment of inertia of concrete core
N_{Ed}	Plastic resistance to compression with considering the buckling
χ	Reduction factor for the buckling curve
$P_{0,AISC}$	Plastic capacity of the section with zero-length strength
N_{AISC}	Nominal axial capacity of a circular CFST columns
P_e	Elastic buckling load
$(EI)_{eff1}$	Effective stiffness of the composite section
K_A	Effective length factor
L_A	Laterally unbraced length of the column
E_{c1}	Modulus of elasticity of concrete
ω	Linear approximator's parameter
e_k	Errors
C	Regularization parameter
y_k	Dependent variables
b	Bias
n	Dataset size
α_k	Lagrange multipliers
RBF	Radial basis functions
$K(x, x_k)$	Kernel function
σ	RBF width
$\vec{X}(t+1)$	Location vector of wolves at iteration $(t+1)$
$\vec{X}_p(t)$	A location vector of prey at iteration t
\vec{A}, \vec{C}	Coefficient vectors
\vec{r}_1, \vec{r}_2	Random vectors of $[0,1]$
RMSE	Root-mean-square error
MAE	Mean absolute error
MAPE	Mean absolute percentage error
R	Correlation coefficient

1 Introduction

Concrete-filled steel tube (CFST) columns are widely used in construction works such as high-building columns and piers due to its superiority compared to traditional reinforced concrete (RC) or absolute steel columns in terms of high strength and ductility, high stiffness, high fire resistance, and large energy dissipation capacity [1, 2]. CFST columns can use concretes with different strengths such as normal strength concrete (NSC), high-strength concrete (HSC), high-strength concrete, or ultra-high-strength concrete (UHSC).

The load acting on the CFST columns usually has two forms: the load acting on the entire steel and concrete (type 1) and the load acting only on the concrete core (type 2) [3]. Specifically, for type 1, the steel tube of the CFST columns plays a role of reinforcing both longitudinal and transverse reinforcement, bearing axial force with a concrete core and creating round stress to the concrete core when expansion deformation of concrete is higher than steel tube. The confinement effect caused by steel pipes increasing the strength and ductility of CSFT columns. For type 2, the load is only applied to the concrete cross section, so the steel tube only bears the axial force along with concrete through the adhesion force of two layers of material and the main effect is to restrain the expansion of concrete core, thereby transmitting round stress into concrete to enhance compressive strength and ductility.

The ultimate bearing capacity (UBC) of the CFST column is a very important factor in the working capacity of the CFST columns. Accurate determination of the UBC of CFST columns is complicated because they are influenced nonlinearly by many factors such as steel tube length (L), steel tube thickness (t), ratio length and diameter of CFST (L/D) columns, steel fiber properties (if any) in concrete and compressive strength of concrete used in CFST columns. Currently, international standards such as Eurocode 4 (EC4), AISC (American standards), ACI 318R (standards of the American concrete association), Chinese standards DLT/5085-1999 have proposed many formulas and different approaches to calculating extreme load capacity. Besides, there have also been many experimental models proposed in previous studies of many authors around the world.

The load capacity or critical compressive strength of CFST columns is a matter of interest to many researchers. There are various empirical and theoretical studies to come up with a formula for predicting the load capacity of the CFST columns [2, 4, 5]. For example, Han et al. presented the advanced applications of CFST structures [1], Gardner et al. studied structural behavior of CFST [6], Goode used 1819 tests on CFST columns and compared to

experimental studies [7]. Besides, Guler et al. also studied axial capacity and ductility of circular UHPC-filled steel tube columns [8] or Liew et al. designed the concrete-filled tubular beam columns with high-strength steel and concrete [9]. In addition, the standards (ACI 318, AISC 2010, AS3600, CECS 28:90, CISC 2007, DBJ 13-51-2003, EC4) also provide specific formulas to calculate the CFST columns load capacity.

Most of the formulas for predicting the extreme strength of CFST columns are only suitable for NSC concrete, in some standards, and studies have also expanded and adjusted for HSC but only up to 90 MPa. The standards are also limited in accurately predicting the strength of CFST columns for all types of concrete strength, especially with UHSC concrete [10]. These studies have not proposed the formula for estimating the UBC of CFST columns covering various types of concretes. Therefore, it is essential and practical to set up a model to predict the UBC of CFST columns using various concrete compressive strengths.

With the explosion of the science and technology network, many new techniques are born, including artificial intelligence (AI). The final goal of AI is to develop human-like intelligence in machines and can be accomplished through learning algorithms which try to mimic how the human brain learns [11]. There are more and more researchers used the application of AI such as predicting of ore crushing-plate lifetimes [12], analyzing automatic image of cutting edge wear by neural network approach [13], or predicting the micro-drilling using multiple sensors using AI-based hole quality [14].

The experimental formula limits the accuracy in predicting the compressive strength of a CFST column due to its simplicity. The AI and machine learning are considered a revolution that can apply for solving real problem in civil structures [15], shear strength prediction in reinforced concrete deep beams [16], energy efficiency [17, 18], predictions of long-term deflections of reinforced concrete structures [15], crack detection [19], building information modeling [20], and prediction of concrete components [21]. Due to its fast learning performance and high reliability, there have been several studies using AI to simulate the behavior of structures and materials help increase predictive accuracy and helps reduce deviations in structural design [22, 23].

The application of AI for predicting the bearing capacity of CFST columns is necessary for designing of the engineering domain. Gholampour et al. applied multivariate adaptive regression splines (MARS), M5 model tree (M5Tree), and support vector regression (SVR) models in evaluating mechanical properties of concretes [24]. Among the AI techniques for regression problems, the SVR is one of the most used models [25]. For example, the SVR models have been applied for evaluating the stiffness of RC

members [26]. In addition, the performance optimization of the SVR models is meaningful in practice. The grey wolf optimization (GWO) algorithm was effective in solving complex optimization problems [27]. Therefore, this study used the SVR model and the GWO algorithm to develop a prediction model for estimating the ultimate bearing capacity in CFST columns.

In this study, the proposed model integrated the SVR with the GWO algorithm in which the GWO aims to automatically fine-tune the SVR parameters. The goal of the study is to create a best model (SVR-GWO) to estimate the ultimate bearing capacity in CFST columns. The proposed model can consider the influencing factors such as the column diameter (D), thickness of steel tube (t), yield stress of steel (f_y), compressive strength of concrete (f_c), column length (L), D/t ratio (D/t) as inputs for the prediction. Details of the proposed SVR-GWO model are described in Sect. 3. The contributions of this study are twofold. The first contribution is to propose an AI-based hybrid prediction model in predicting the bearing capacity of CFST columns. The second contribution is to promote and highlight AI applications in the civil engineering domain.

2 Literature review

2.1 Relevant studies

Normally, the CFST columns are divided into three types based on the length/diameter (L/D) ratio of the column: short column (if $L/D \leq 4$); medium columns (if $4 < L/D \leq 12$) and thin column (if $L/D \geq 12$)—this is a standard classification of Japanese AIJ 2001. Many studies have shown that the strength of columns reduces when increasing the L/D ratio. Moreover, the load capacity also depends on the diameter/thickness ratio of steel tube (D/t), the tensile strength of steel pipe, concrete strength, additional load on steel core or on the whole section. According to researches, the load strength increases when the ratio of D/t decreases or the tensile steel strength increases [2, 28].

The load strength in CFST columns mainly is influenced by the expansion confinement of the steel tube. Accordingly, when adding load on a concrete core, steel tube works as expansion material confinement inside the concrete core; therefore, it yields a higher load capacity than the case of additional load on the whole section when the steel tube has both vertical and round stresses making the expansion stress decreases [5, 29].

Recently, an important issue that studies mention is the effect of concrete strength. Liew et al. [9], Tue et al. [30], and Uy et al. [28] showed that when the concrete strength raised, the expansion confinement reduced because of the

higher the strength of concrete, the lower the coefficient of expansion compared to the lower concrete capacity. With CFST columns, research by An and Fehling [3] showed that the design criteria for predicting the load were higher than the actual test of CFST columns, especially those using concrete strength higher than 90 MPa. On the other hand, there is various concrete with different aggregates as well as properties and affects loads such as light weight reinforced concrete, fibrous concrete, recycled concrete. Hence, it is important to study CFST columns using different concrete, high-strength, and ultra-high-strength concrete and proposing a formula for calculating the load capacity for this column is necessary.

Ahmadi et al. [31] introduced the artificial intelligence (AI) approach to forecast compressive concrete strengths of round-section CFST columns with different column parameters. In this model, the compressive concrete strength was reached to 106 MPa and the yield strength of steel tube was 853 MPa. Jayalekshmi et al. [32] introduced the load capacity of round-section CFST columns formulation using the AI approach and compared with the predicted models of the previous researches.

Du et al. [33] used the AI method to calculate the critical compression strength of rectangular section CFST columns based on 305 experimental results and compared with predictions from European standards EC4, standards of American ACI concrete, Chinese standard GJB4142, and American AISC360-10 steel Association standard. In addition to this, Du et al. [33] used AI to examine effects of column parameters such as the yield strength steel tube, steel tube thickness, concrete strength, the height/diameter ratio of the column to the strength, and ductility of columns.

Recently, Linh et al. [34] used 300 axial compression test samples on square section CFST columns to propose an empirical formula for calculating vertical load capacity based on the artificial neural networks (ANNs) model. The author observed that the formulas given from ANNs had more accurate results than those of other authors and the existing design standards. The ANNs model was also applied for predicting the flutter velocity of suspension bridges [35].

Sarir et al. [36] based on the advanced methods including gene expression programming (GEP) according to the decision tree algorithm, ensemble models including ANN and optimized algorithm (particle swarm optimization—PSO) to build a prediction model for predicting the load capacity of CFST columns and optimizing this model. In addition, the authors compared the GEP, ANNs, and PSO methods and showed that the GEP method had the best predictive results and yielded the best regression coefficients.

Karatas [37] used the MARS method to establish a formula for the bearing capacity of the CFST columns. Nour and Guneyisi [38] based on 97 experimental samples and used genetic algorithms (GA) to develop the formula for predicting the bearing capacity for short columns (L/D from 2 to 3.5). The CFST columns in their study used recycled aggregate. They then compared the calculated load capacity from the new formula with the predicted values from the design standards and showed that the new formula based on the genetic algorithm had high accuracy.

Ahmadi et al. [39] also investigated the load capacity of round-section CFST columns by using AI for a large number of tested samples and compared with five previously predicted models. Similar results could be found in the studies of Jegadesh and Jayalekshmi [32], Liu [40], Güneysi et al. [41]. Therefore, over-viewing the number of studies using AI to assess the bearing capacity of the CFST columns is very limited. Furthermore, previous studies just focused on columns using concrete cores of normal compressive strength (< 50 MPa) or high (50–90 MPa), and there have been no studies related to columns using ultra-high reinforced concrete strength (> 90 MPa). Thus, this study aims to research CFST columns samples with different compressive strength of concrete cores.

2.2 Empirical methods for CFST columns

This section describes two popular empirical methods for calculating the bearing capacity of CFST columns that are the Euro code 4 [42] and American code AISC 2010 [43]. For CFST columns, these two codes are usually used by engineers in design, which are detailed as below.

2.2.1 Euro Code 4 (EN 1994-1-1:2004) (EC4)

Confinement effect is considered for concrete-filled circular tubes with relative slenderness $\bar{\lambda}$ not larger than 0.5 and the ratio of eccentricity to diameter e/D less than 0.1, and then, the plastic cross-sectional resistance under compression can be determined as [42]:

$$N_{pl,Rd} = \eta_a A_s f_y + A_c f_c \left(1 + \eta_c \frac{t f_y}{D f_{ck}} \right) \quad (1)$$

in which

$$\eta_c = 4.9 - 18.5 \bar{\lambda} + 17 \bar{\lambda}^2 \quad (\eta_c \geq 0) \quad (2)$$

$$\eta_a = 0.25(3 + 2 \bar{\lambda}) \quad (\eta_a \leq 1) \quad (3)$$

$$\bar{\lambda} = \sqrt{\frac{N_{pl,Rk}}{N_{cr}}} \quad (4)$$

$$N_{pl,Rk} = f_y A_s + 0.85 f_c A_c \quad (5)$$

$$N_{cr} = \frac{\pi^2(EI)_{eff}}{l^2} \tag{6}$$

$$(EI)_{eff} = E_s I_s + K_e E_{c2} I_c \tag{7}$$

η_c is the confinement coefficient of concretes; η_a is the confinement coefficient of steel tubes; f_y is the yield strength of the steel, f_c is the unconfined concrete compressive strength, A_s and A_c are the section areas of the steel and concrete, respectively; N_{cr} is the elastic critical normal force for the relevant buckling mode; $(EI)_{eff}$ is the effective flexural stiffness for calculation of relative slenderness; I_s and I_c are the moment of inertia of steel tube and concrete core, respectively.

K_e is the correction factor that should be taken as 0.6, and l is the buckling length of the CFST columns, and E_{c2} is the concrete elastic modulus.

The plastic resistance to compression with considering the buckling is given by:

$$N_{Ed} = \chi N_{pl,Rd} \tag{8}$$

where χ is the reduction factor for the buckling curve

$$\chi = \frac{1}{\phi + \sqrt{\phi^2 - \lambda^2}} \tag{9}$$

$$\phi = 0.5 [1 + 0.21(\bar{\lambda} - 0.2) + \bar{\lambda}^2] \tag{10}$$

Some limitations of EC4 (2004) can be given as follows:

- The code is limited to structural steel grades S235 to S460 and normal weight concrete of strength classes C20/25 to C50/60.
- The steel contribution ratio δ should follow the condition: $0.2 \leq \delta \leq 0.9$, where

$$\delta = \frac{A_s f_y}{N_{pl,Rd}} \tag{11}$$

- The local buckling could be neglected with the maximum value D/t

$$\max(D/t) = 90 \frac{235}{f_y} \tag{12}$$

- The relative slenderness $\bar{\lambda}$ should not exceed 2.0. The ratio of the depth to the width of the composite cross section should be within the limits of 0.2 and 5.0

2.2.2 American Code AISC 2010 (AISC)

For circular CFST columns, the AISC [43] has considered the concrete confinement through the hoop stress in steel

tube (using coefficient 0.95), and the cross-sectional strength $P_{0,AISC}$ is given by [43]:

$$P_{0,AISC} = 0.95 f_c A_c + f_y A_s \tag{13}$$

$P_{0,AISC}$ is defined as the plastic capacity of the section with zero-length strength. f_y is the yield strength of the steel, f_c is the unconfined concrete compressive strength, A_s and A_c are the section areas of the steel and concrete, respectively. Therefore, to consider the length effects of the column, the nominal axial capacity of a circular CFST column is calculated by:

$$N_{AISC} = \begin{cases} P_{0,AISC} \left[0.658 \left(\frac{P_{0,AISC}}{P_e} \right) \right] & (P_e \geq 0.44 P_{0,AISC}) \\ 0.877 P_e & (P_e < 0.44 P_{0,AISC}) \end{cases} \tag{14}$$

where P_e is the elastic buckling load and is given by:

$$P_e = \frac{\pi^2 (EI)_{eff1}}{(K_A L_A)^2} \tag{15}$$

in which $(EI)_{eff1}$ is the effective stiffness of the composite section

$$(EI)_{eff1} = E_s I_s + C_3 E_{c1} I_c \tag{16}$$

$$C_3 = 0.6 + 2 \left(\frac{A_s}{A_c + A_s} \right) \tag{17}$$

K_A is the effective length factor; L_A is the laterally unbraced length of the column; I_s and I_c are the moment of inertia of steel tube and concrete core, respectively; E_{c1} is the modulus of elasticity of concrete

Some limitations of AISC (2010) are shown as below:

- The code is limited to structural steel yielding strength up to 525 MPa, normal weight concrete of cylinder strength from 21 to 70 MPa, and lightweight concrete of cylinder strength from 21 to 42 MPa
- Limitation of the diameter-to-thickness ratio of circular CFST column is given by:

$$\begin{aligned} \max(D/t) &= \frac{0.15 E_s}{f_y} && \text{for compact/noncompact} \\ \max(D/t) &= \frac{0.19 E_s}{f_y} && \text{for compact/slender} \end{aligned} \tag{18}$$

Higher ratios are permitted when their use is justified by testing or analysis

- The cross-sectional area of the steel core shall comprise at least 1% of the total composite cross section.

3 Hybrid AI-based prediction model

3.1 Support vector regression for bearing capacity of CFST columns

The support vector regression (SVR) [44] is a supervised learning model belonging to machine learning, that is used for regression problems. It has been used for capturing the nonlinear relationship between the predictors and dependent variables. Figure 1 demonstrates a framework of the SVR model. It uses a kernel function to map predictors to high-dimension feature space. A least-squares cost function is applied to train an SVR model to yield linear equations in a dual space that reduces computing time. Particularly, SVR models are taught by solving Eq. (19).

$$\min_{\omega, b, e} J(\omega, b, e) = \frac{1}{2} \|\omega\|^2 + \frac{1}{2} C \sum_{k=1}^n e_k^2; \tag{19}$$

subject to $y_k = \langle \omega, \phi(x_k) \rangle + b + e_k, \quad k = 1, \dots, n$

where $J(\omega, b, e)$ is an objective function; ω is a linear approximator’s parameter; e_k is errors; $C \geq 0$ is a regularization parameter; x_k is predictors; y_k is dependent variables (i.e., the ultimate bearing capacity of CFST columns in this study); b is bias; and n is the dataset size.

Lagrange multipliers (α_k) are utilized for dealing with this problem that results in Eq. (20). A kernel function is described in Eq. (21). Among the kernel function, the Gaussian radial basis functions (RBF) kernel is powerful and is applied in this study as presented in Eq. (22).

$$f(x) = \sum_{k=1}^n \alpha_k K(x, x_k) + b \tag{20}$$

$$K(x, x_k) = \sum_{k=1}^n g_k(x) g_k(x_k) \tag{21}$$

$$K(x, x_k) = \exp(-\|x - x_k\|^2 / 2\sigma^2) \tag{22}$$

where α_k is Lagrange multipliers; $K(x, x_k)$ is the kernel function; σ is the RBF width.

Performance of SVR models is affected by the value settings of its hyperparameters that consist of the RBF width (σ) and the regularization parameter (C). In this study, the optimal settings of these two hyperparameters were considered comprehensively. Particularly, a recently developed metaheuristic grey wolf optimization (GWO) algorithm [27] was integrated to optimize the performance of the proposed AI model. The mathematical theory of GWO was presented in the next section.

3.2 Grey wolf optimization for improving performance of AI model

The GWO is a metaheuristic optimization algorithm [27] that inspires the natural behaviors of grey wolves. The GWO follows the power hierarchy and hunting activities of wolves. Particularly, a swarm of grey wolves is split hierarchically into four subswarms of alphas (α), beta (β), delta (δ), and omega (ω) in which power and responsibility of each group are different.

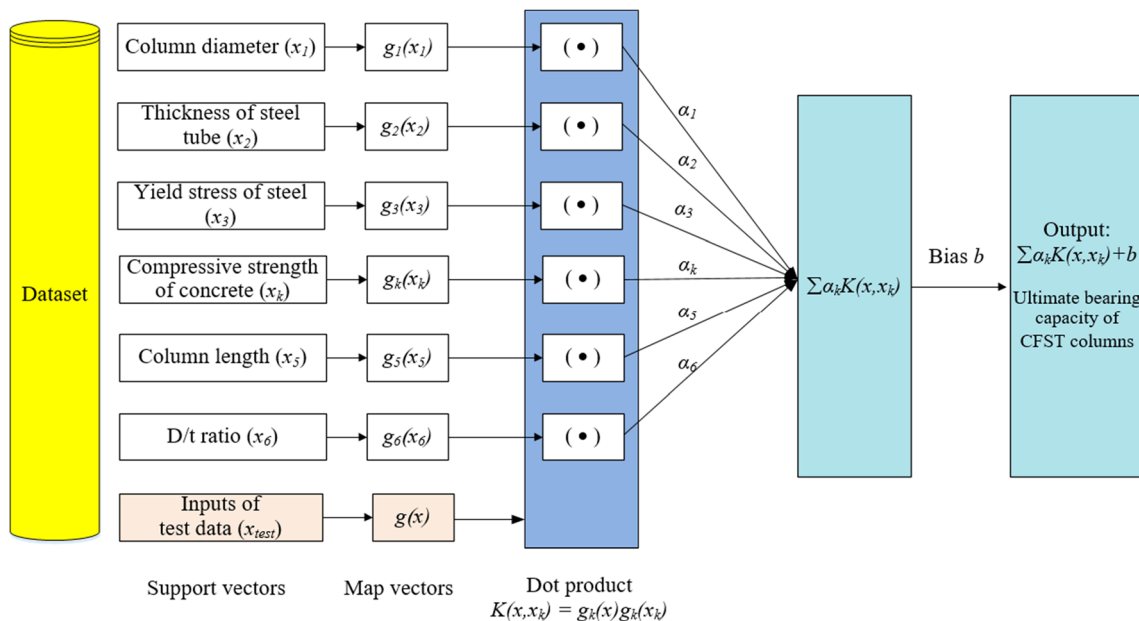


Fig. 1 The framework of support vector regression

Fig. 2 Pseudo-code of the grey wolf optimization

```

Initializing a population of grey wolf  $X_i$  ( $i = 1, 2, \dots, m$ )
Setting the coefficient vector  $\vec{a}$ 
Calculating  $A$ , and  $C$  (.)
Calculate the fitness of all wolves
 $X_\alpha$  is the best wolf,  $X_\beta$  is the second-best wolf,  $X_\delta$  is the third best wolf
while (the stopping criteria is not satisfied)
    for each wolf
        Updating the location of the wolf by Eq. (28)
    end for
    Updating  $a$ ,  $A$ , and  $C$ 
    Calculating the fitness of all search wolf
    Update  $X_\alpha$ ,  $X_\beta$ , and  $X_\delta$ 
     $t = t + 1$ 
end while
return  $X_\alpha$ 
    
```

Table 1 Descriptive analysis of data attributes

Statistical values	Data attributes						
	Column diameter D (mm)	Thickness of steel tube T (mm)	Yield stress of steel F_y (N/mm ²)	Compressive strength of concrete F_c (N/mm ²)	Column length L (mm)	D/t ratio D/t	Ultimate bearing capacity of CFST column N_u (kN)
Average	174.35	4.42	359.42	62.87	506.05	48.62	3095.70
Std. dev.	109.74	2.46	111.23	37.11	313.97	34.23	4476.56
Min	48.00	0.52	181.40	9.90	150.00	9.00	106.00
Max	1020.00	16.54	853.00	193.30	3060.00	220.93	46000.00

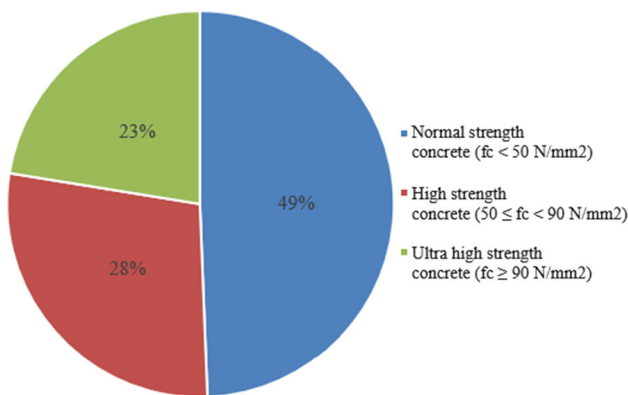


Fig. 3 Proportion of three different strength concretes

- Alpha is a leader.
- Beta is subordinate wolves that consult the alpha and manage the pack

- Delta is wolves that need to report to the alpha and betas.
- Omega plays as a scapegoat and reports to the alpha, beta, and delta.

For modeling the social power of wolves, the α is considered as the fittest solution, and β and δ are considered as the 2nd and 3rd third best solutions, respectively. The optimization by the GWO includes searching, encircling, and attacking prey. The hunting process is led by α , β , and δ . Encircling prey was performed by updating the wolf position by using by Eq. (23). Three of them were used to predict the location of the grey, while the location of omegas was updated randomly surrounding the three best wolves as shown in Eqs. (25)–(28) [27].

$$\vec{X}(t + 1) = \vec{X}_p(t) - \vec{A} \cdot \left| \vec{C} \cdot \vec{X}_p(t) - \vec{X}_p(t) \right| \tag{23}$$

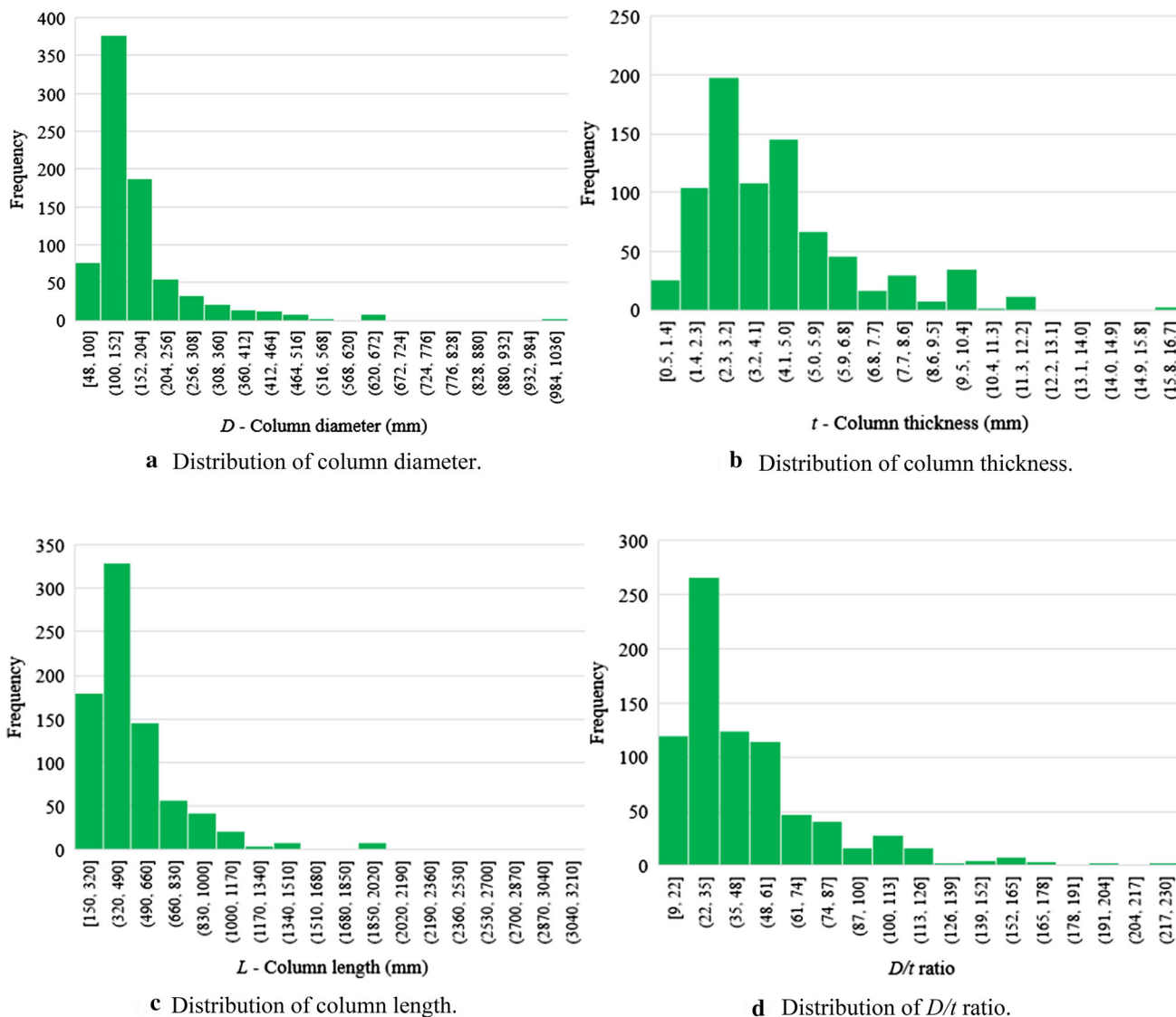


Fig. 4 Distribution of column geometry attributes

$$\vec{A} = 2\vec{a} \cdot \vec{r}_1 - \vec{a} \quad \text{and} \quad \vec{C} = 2 \cdot \vec{r}_2 \tag{24}$$

$$\vec{X}_1 = \vec{X}_\alpha - \vec{A}_1 \cdot \left| \vec{C}_1 \cdot \vec{X}_\alpha - \vec{X} \right|, \tag{25}$$

$$\vec{X}_2 = \vec{X}_\beta - \vec{A}_2 \cdot \left| \vec{C}_2 \cdot \vec{X}_\beta - \vec{X} \right| \tag{26}$$

$$\vec{X}_3 = \vec{X}_\delta - \vec{A}_3 \cdot \left| \vec{C}_3 \cdot \vec{X}_\delta - \vec{X} \right| \tag{27}$$

$$\vec{X}(t+1) = \frac{\vec{X}_1 + \vec{X}_2 + \vec{X}_3}{3} \tag{28}$$

where $\vec{X}(t+1)$ is a location vector of wolves at iteration $(t+1)$; $\vec{X}_p(t)$ is a location vector of prey at iteration t ; \vec{A} and \vec{C} are coefficient vectors; \vec{a} are reduced from 2 to 0 through iterations; \vec{r}_1 and \vec{r}_2 are random vectors of $[0,1]$.

The diversity of exploitation and exploration in the GWO was controlled by the vector \vec{A} . During the optimization process, when $|A| < 1$, the wolves tend to approach the prey because the next location of wolves is in the area between their current locations and the prey’s position. This conforms the exploitation of the GWO.

In contrast, as $|A| > 1$, wolves tend to diverge from the prey that confirms the global exploration. Besides, the vector \vec{C} influences on the exploration and exploitation of the GWO because it is a random weight that affects the update of wolf location as shown in Eq. (25). This helps the GWO to overcome local optima. Figure 2 shows a pseudo-code of the GWO.

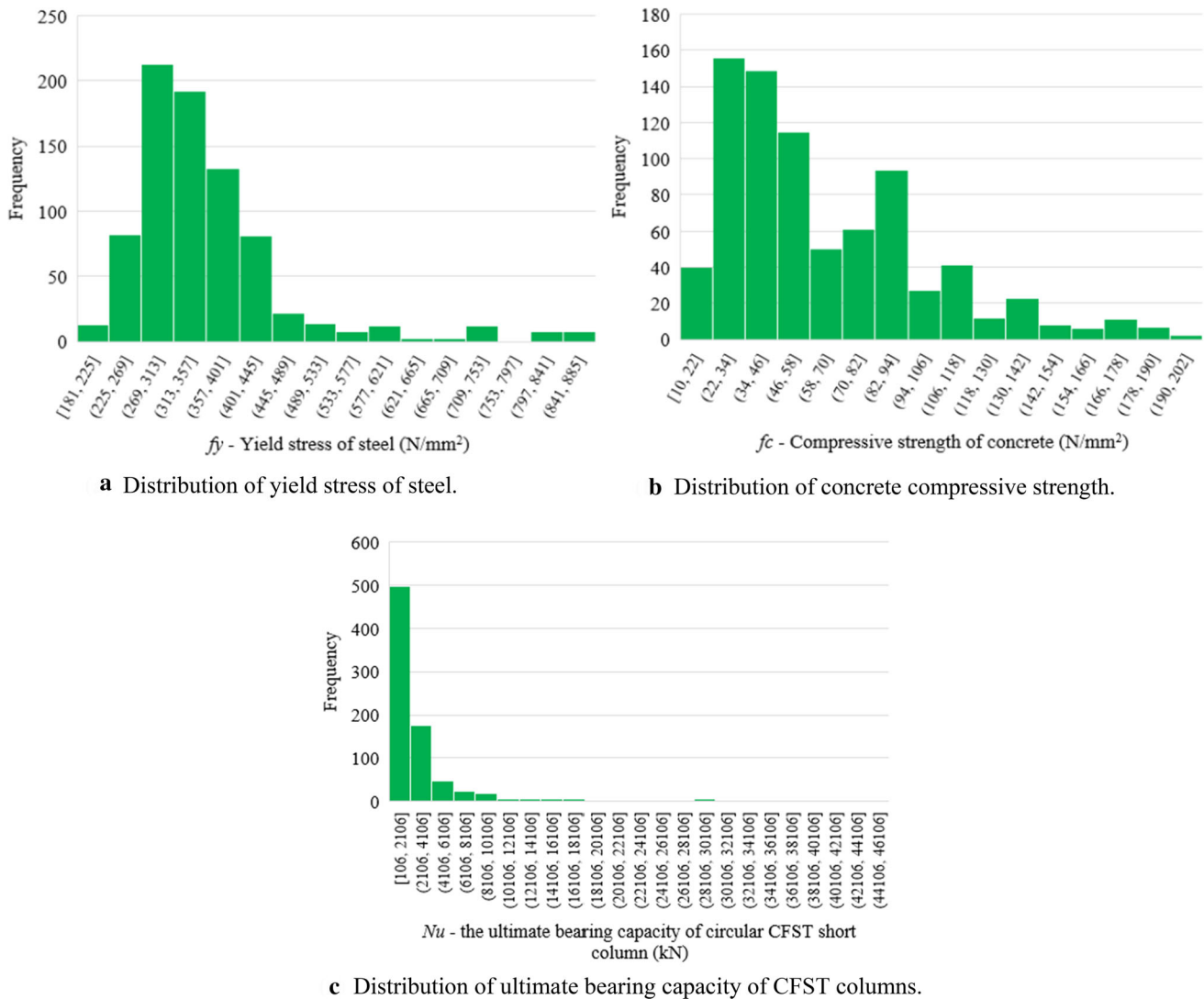


Fig. 5 Distribution of column materials and bearing capacity of CFST columns

4 Results

4.1 Database

A large dataset was collected in this study to evaluate the proposed AI prediction technique that consists of 802 samples of experimental tests circular CFST short columns. The dataset was derived from the Association of Steel–Concrete Composite Structures [45]. Table 1 presents the descriptive analysis of data attributes in the dataset that includes the column diameter (D), thickness of steel tube (t), yield stress of steel (f_y), compressive strength of concrete (f_c), column length (L), D/t ratio (D/t), and ultimate bearing capacity of CFST columns (N_u). For examples, the average diameter of CFST columns was 174.35 mm with a standard deviation of 19.74 mm and the average thickness

of steel tubes ranged from 0.52 to 16.54 mm. The yield stress of steel used in the CFST columns varied widely from 181.40 to 853.00 N/mm².

The used concretes in the experiments consist of the NSC, HSC, and UHSC. Their proportions are shown in Fig. 3 in which the CFST columns with the NSC account for 49% and those of HSC and UHSC account for 23% and 28%, respectively. The average UBC of CFST columns in the dataset was 3095.70 kN with the standard deviation of 4476.56 kN that reveals the wide range of N_u . To provide readers with graphical information, Figs. 4 and 5 visualize the distributions of column geometry attributes and column materials and bearing capacity of CFST columns, respectively. Six attributes related to column geometry and materials were used as input data for the AI prediction model that consists of D , t , f_y , f_c , L , D/t . The output of the

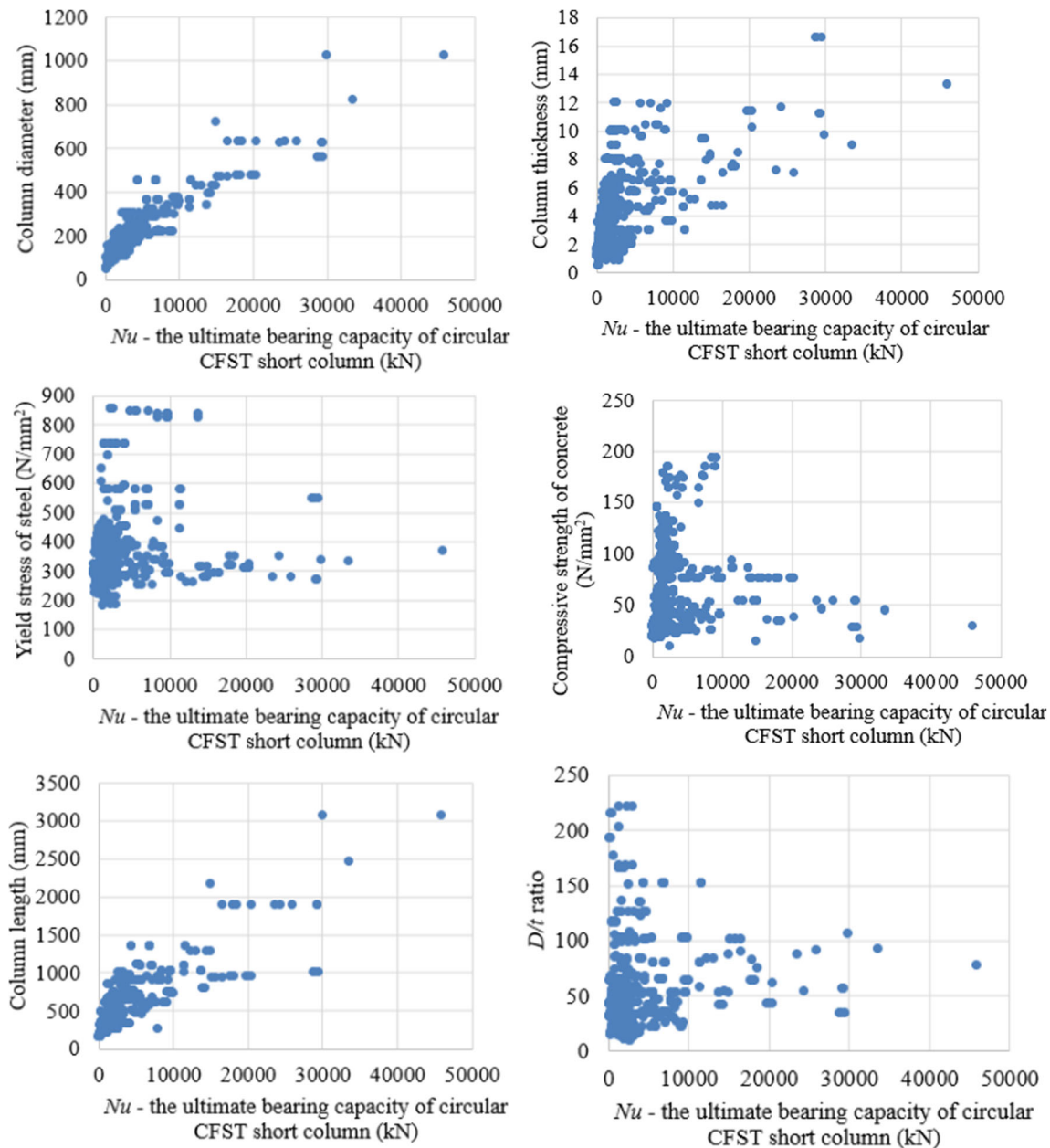


Fig. 6 Scatter plots of CFST columns attributes and ultimate bearing capacity

model was N_u . Figure 6 provides the scatter plots of six above-mentioned inputs and the UBC in the dataset.

4.2 Evaluation process

The evaluation process is the learning phase and the test phase in which the experimental dataset of 802 samples of CFST columns was split randomly to the learning dataset and the test dataset. Figure 7 presents data processing for the model evaluation process. The learning dataset was to train and optimize the AI models, which accounts for 90% of the sample size of the original dataset. In the learning

phase, the AI model was trained by using the training data that account for 70% of the learning database. In total, 30% of the learning database was used as the validating data to optimize the AI models by fine-tuning the hyperparameters of the AI models. Meanwhile, the test dataset aimed to test the performance of the trained and optimized AI models for predicting the UBC of circular CFST short columns.

The optimal configuration of the SVR-GWO model was defined by the values of hyperparameters C and σ . As shown in Fig. 7, the GWO algorithm was to optimize the configuration of the SVR-GWO model by minimizing the objective function which was the root-mean-square error

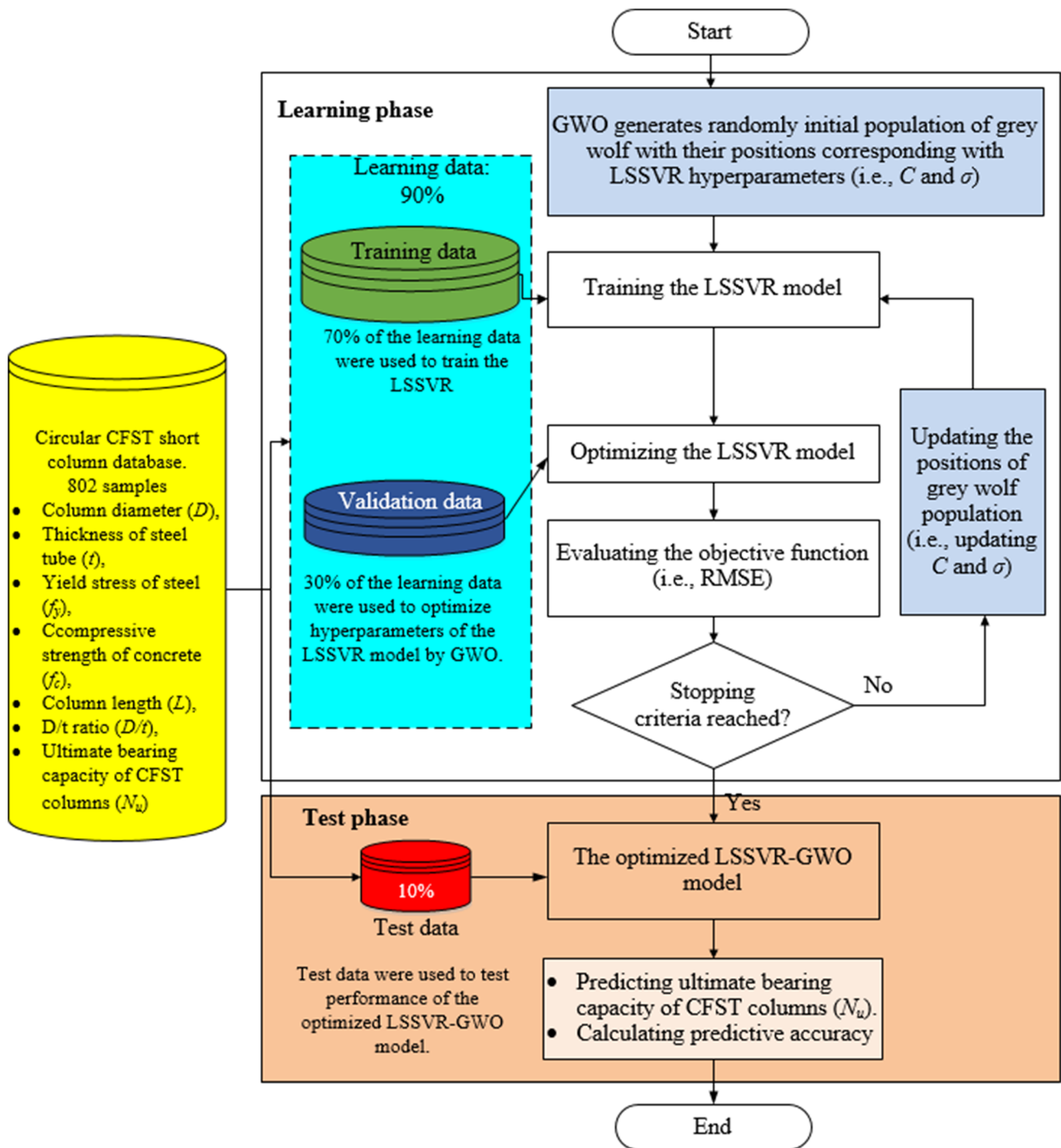


Fig. 7 Evaluation process for predicting ultimate bearing capacity of CFST columns

(RMSE). Table 2 shows the settings of the SVR-GWO model. The search space was set from 0.001 to 1000. The RBF was used as the kernel function in the SVR model. The GWO population was set as 100, and the maximum iteration was 10. The GWO was generated initially by the population of the grey wolf in which their coordinates represented the C and σ values in the search space. The

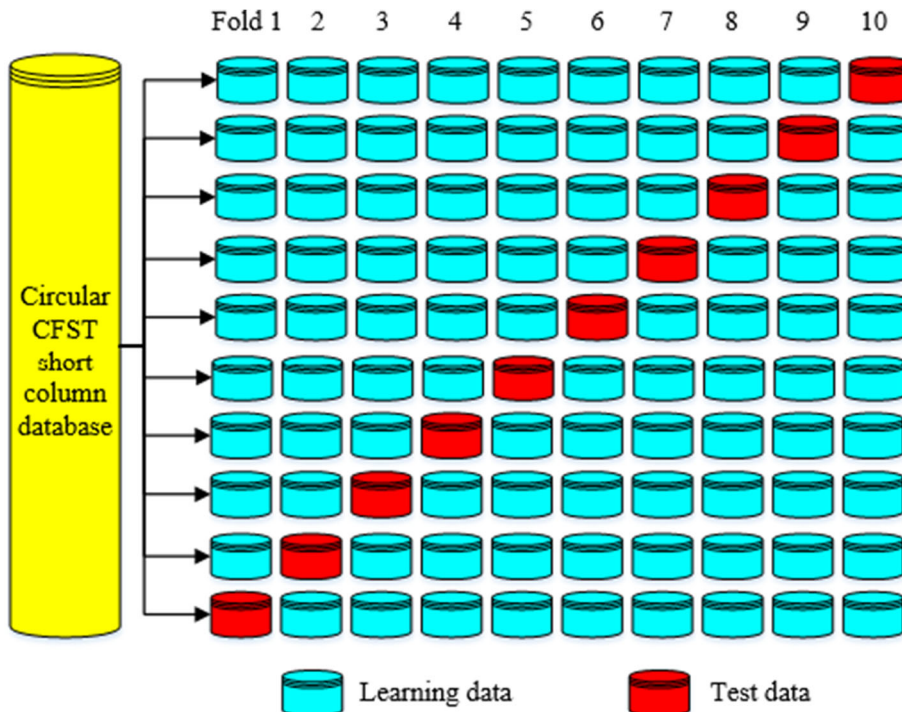
optimal configuration was reached as stopping criteria were satisfied. The SVR-GWO model was implemented in MATLAB programming language.

To ensure the generalizability in the model evaluation, the AI models were evaluated 10 times with the aid of a k -fold cross-validation method. The original database was split with tenfold as shown in Fig. 8. In each evaluation,

Table 2 Settings for the GWO-SVR model

Model	Parameter	Value
Support vector regression	Regularization parameter C	0.001–1000
	RFB width σ	0.001–1000
	Kernel function	Radial basis functions RBF
Grey wolf optimization algorithm	Number of wolves	100
	Maximum iteration	10

Fig. 8 k -fold cross-validation method for evaluation process



the model was learnt by ninefold, while the last fold was to test the accuracy of the learned model. This process was repeated ten times to ensure the model’s generalizability.

4.3 Evaluation indices

Model performance is assessed via statistical indices that consist of RMSE [Eq. (29)], mean absolute error (MAE) [Eq. (30)], mean absolute percentage error (MAPE) [Eq. (31)], and correlation coefficient (R) [Eq. (32)]. Higher R , lower MAE, RMSE, and MAPE indicate good predictive performance.

$$RMSE = \sqrt{\frac{1}{n} \sum_{i=1}^n (y - y')^2} \tag{29}$$

$$MAE = \frac{1}{n} \sum_{i=1}^n |y - y'| \tag{30}$$

$$MAPE = \frac{1}{n} \sum_{i=1}^n \left| \frac{y - y'}{y} \right| \tag{31}$$

$$R = \frac{n \sum y \cdot y' - (\sum y)(\sum y')}{\sqrt{n(\sum y^2) - (\sum y)^2} \sqrt{n(\sum y'^2) - (\sum y')^2}} \tag{32}$$

where y' is predicted data; y is actual data; and n is database size.

4.4 Analytical results

The result section shows evaluation results of the proposed SVR-GWO model for predicting the UBC in circular CFST columns through the learning and test phases. The comparison among the proposed model with other AI models and empirical methods was also presented in this section.

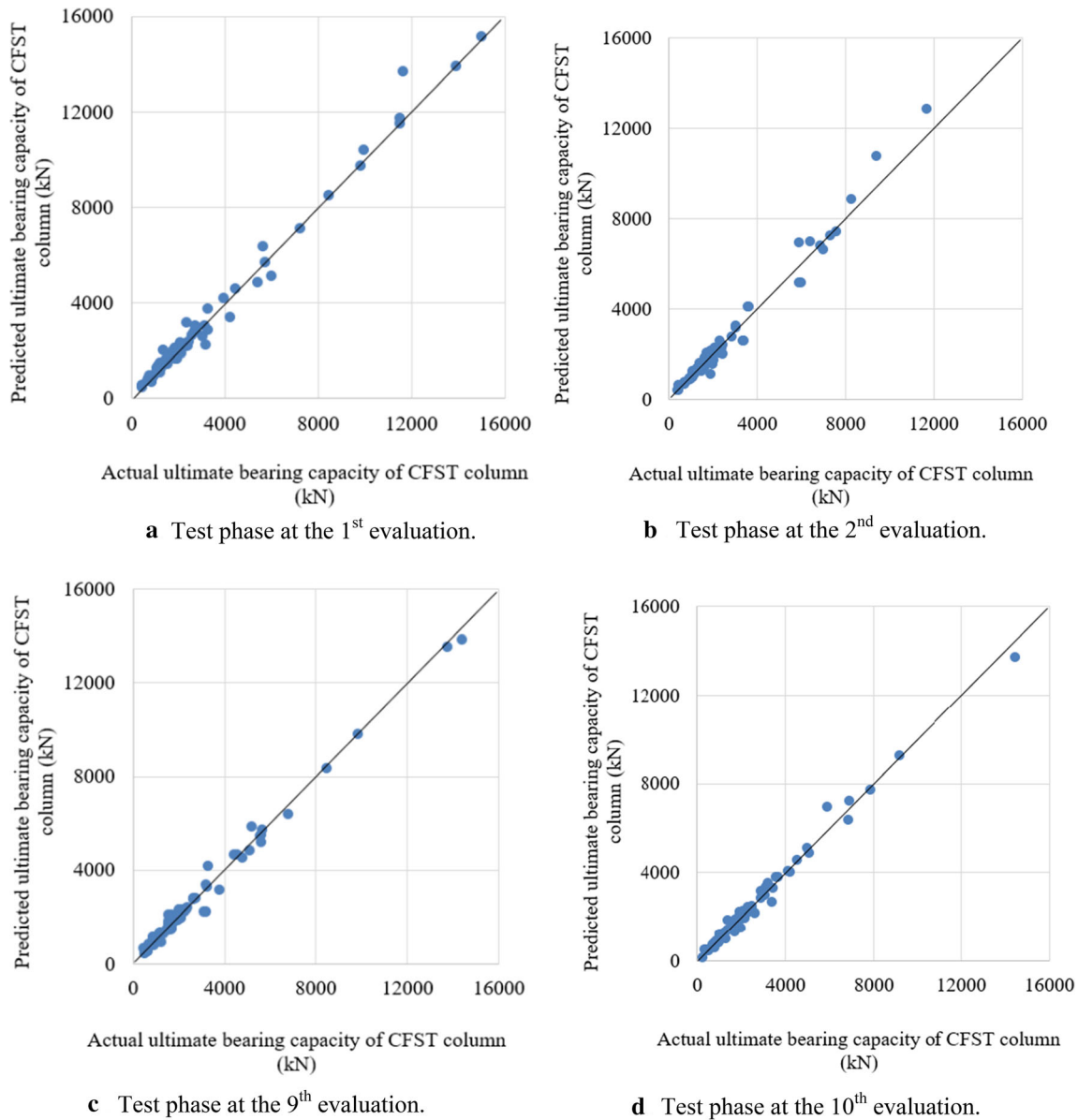


Fig. 9 Actual and predicted ultimate bearing capacity of CFST columns by the hybrid AI model

4.4.1 Evaluation results

Figure 9 presents a comparison of actual values and predicted the UBC of CFST columns by the hybrid AI model. The scatter points in four evaluations in Fig. 9 were very close to the diagonal line that reveals the strong agreement between the experimental results of the CFST column test and predicted values produced by the SVR-GWO model. Table 3 depicts the predictive accuracy of the model in ten evaluation through the learning phase and test phase. Particularly, the predictive accuracy was assessed by the RMSE, MAE, MAPE, and R.

In the learning phase, the average accuracy of the SVR-GWO model in the prediction was 277.11 kN in the RMSE, 174.41 kN in the MAE, 8.25% in the MAPE, and 0.998 in R. The proposed model also obtained a competitive accuracy in the test phase. Particularly, the MAPE reached 9.07% on average and 1.69% in standard deviation, while the *R*-value was 0.994 which was extremely close to 1. The results confirmed the effectiveness of the SVR-GWO model in the UBC prediction of circular CFST columns with considering various concretes of NSC, HSC, and UHSC.

To improve the readability, Fig. 10 charts the MAPE and R comparisons across tenfold cross-evaluation.

Table 3 Predictive accuracy of the hybrid AI model in training and test phases

Evaluation	RMSE_Tr (kN)	RMSE_Te (kN)	MAE_Tr (kN)	MAE_Te (kN)	MAPE_Tr (%)	MAPE_Te (%)	R_Tr	R_Te
1	273.76	359.52	172.35	207.48	8.15	8.47	0.998	0.994
2	262.83	403.12	166.39	239.97	8.07	8.15	0.998	0.995
3	370.26	365.38	219.41	213.36	10.56	13.70	0.996	0.998
4	276.21	309.01	175.63	170.20	8.04	8.03	0.998	0.996
5	266.31	996.01	168.62	274.86	7.89	9.47	0.998	0.991
6	254.13	471.15	162.03	256.27	7.74	8.43	0.998	0.997
7	274.40	327.28	174.04	203.81	8.12	8.73	0.998	0.996
8	238.75	1521.16	155.39	409.51	7.81	9.22	0.998	0.977
9	280.12	267.20	177.50	171.97	8.19	8.43	0.998	0.995
10	274.31	238.29	172.75	154.70	7.96	8.12	0.998	0.997
Average	277.11	525.81	174.41	230.21	8.25	9.07	0.998	0.994
Min.	238.75	238.29	155.39	154.70	7.74	8.03	0.996	0.977
Max.	370.26	1521.16	219.41	409.51	10.56	13.70	0.998	0.998
Std.	35.02	410.85	17.18	73.87	0.82	1.69	0.001	0.006

Tr stands for training, and Te stands for test

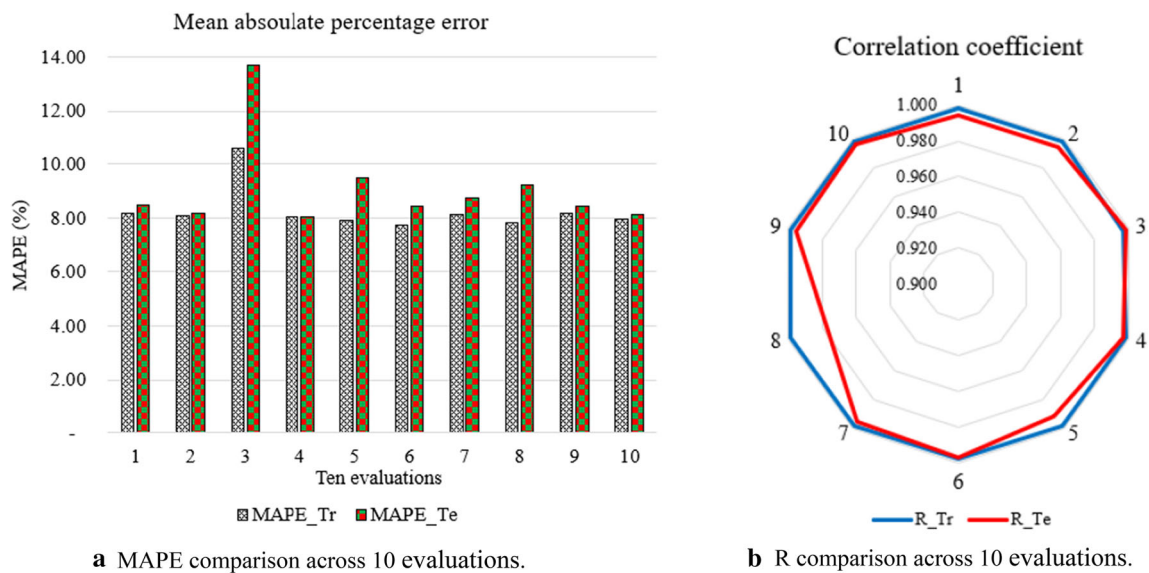


Fig. 10 Predictive accuracy of the hybrid SVR-GWO model in learning and test phases

Table 4 Optimal hyperparameters of hybrid SVR-GWO model over the tenfold cross-evaluation process

Hyperparameters of hybrid SVR-GWO model	Optimal hyperparameters of hybrid SVR-GWO model over tenfold cross-evaluation process									
	1	2	3	4	5	6	7	8	9	10
C	1000	1000	1000	1000	1000	1000	1000	1000	1000	1000
σ	26.24	23.71	79.19	25.80	21.59	23.44	26.39	19.85	26.86	22.38

Table 5 Parameter settings of compared AI models

Model	LR	ANNs	SVR
Settings	attributeSelectionMethod = M5 method ridge = 1.0×10^{-12}	HiddenLayer = a (i.e., 4) LearningRate = 0.3 Momentum = 0.2 TrainingTime = 500	$C = 1$ RBFKernel function gamma = 0.01 Epsilon = 1.0×10^{-12}

Table 6 Performance improvement by the hybrid AI model compared to other models

AI model	Average accuracy for prediction				Enhanced accuracy by proposed model (%)			
	R	RMSE (kN)	MAE (kN)	MAPE (%)	R	RMSE	MAE	MAPE
LR	0.943	1488.69	893.70	75.10	5.4 ^a	64.7 ^a	74.2 ^a	87.9 ^a
ANNs	0.980	890.60	610.44	40.26	1.4 ^a	41.0 ^b	62.3 ^a	77.5 ^a
SVR	0.927	2599.82	892.29	27.74	7.2 ^a	79.8 ^a	74.2 ^a	67.3 ^a
EC4	0.992	571.24	272.08	10.12	0.2	8.0	15.4 ^c	10.3 ^b
AISC	0.990	1191.71	587.49	19.71	0.4 ^b	55.9 ^a	60.8 ^a	54.0 ^a
SVR-GWO	0.994	525.81	230.21	9.07				

LR is linear regression; ANNs is artificial neural networks; SVR is support vector regression; EC4 is Euro code 4; and AISC is American code AISC 2005. “a” indicates the level of significance of less than 1%; “b” indicates the level of significance of less than 5%; and “c” indicates the level of significance of less than 10%. Bold values indicate the outperformance among compared models

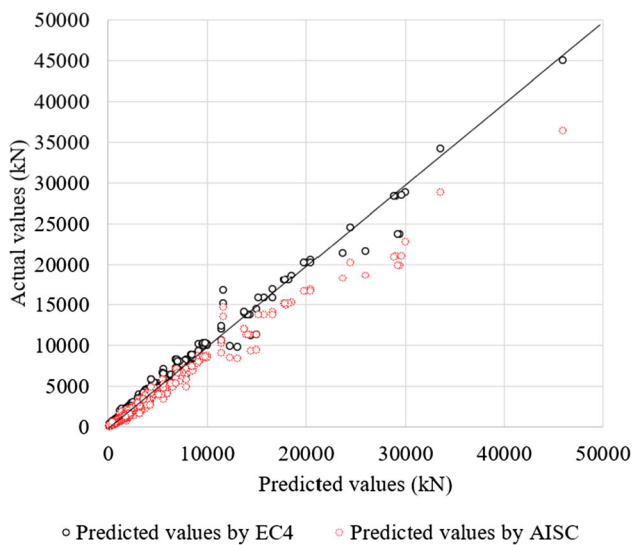


Fig. 11 Actual and predicted bearing capacity of CFST columns by the empirical methods

Figure 10 reveals that most MAPE values in the evaluation process were less than 10% except the 3rd evaluation and the correlation coefficient R values were higher than 0.970 that confirmed the predictability of the proposed model. To provide readers with reference for setting the prediction model, Table 4 reports the optimal results of the model’s hyperparameters which were derived from the optimization by the GWO.

4.4.2 Comparison results

This section aims to compare the proposed AI model and baseline AI models (i.e., LR, ANNs, and SVR models) and the empirical methods (i.e., EC4 and AISC codes). These baseline AI models are effective for prediction tasks [46]. The SVR was proposed by Vapnik [47], and its mathematical theory was presented in [47, 48]. The ANNs model is an effective technique that has been commonly used in the engineering domain. The architecture of an ANNs includes an input layer, one, or more hidden layers of computational nodes, and an output layer. Its theory was presented in [49]. LR models develop the linear relationship between inputs and output as explained in [50]. These models were implemented in the Weka which is an open-source machine learning software [51]. The settings of baseline AI models are presented in Table 5 as default values in the Weka.

Table 6 summarizes the comparison results that reveal performance improvement by the hybrid AI model compared to other models and empirical methods in terms of the four statistical indices. The LR model obtained the low accuracy in the prediction with the high MAPE of 75.10% and MAE of 893.79 kN. The LR model was poor for the nonlinear and complex prediction because it is suitable for capturing a linear relationship between inputs and outputs.

The ANNs and SVR models enable to capture the nonlinear relationship between the characteristics of CFST columns and the bearing capacity of the CFST columns.

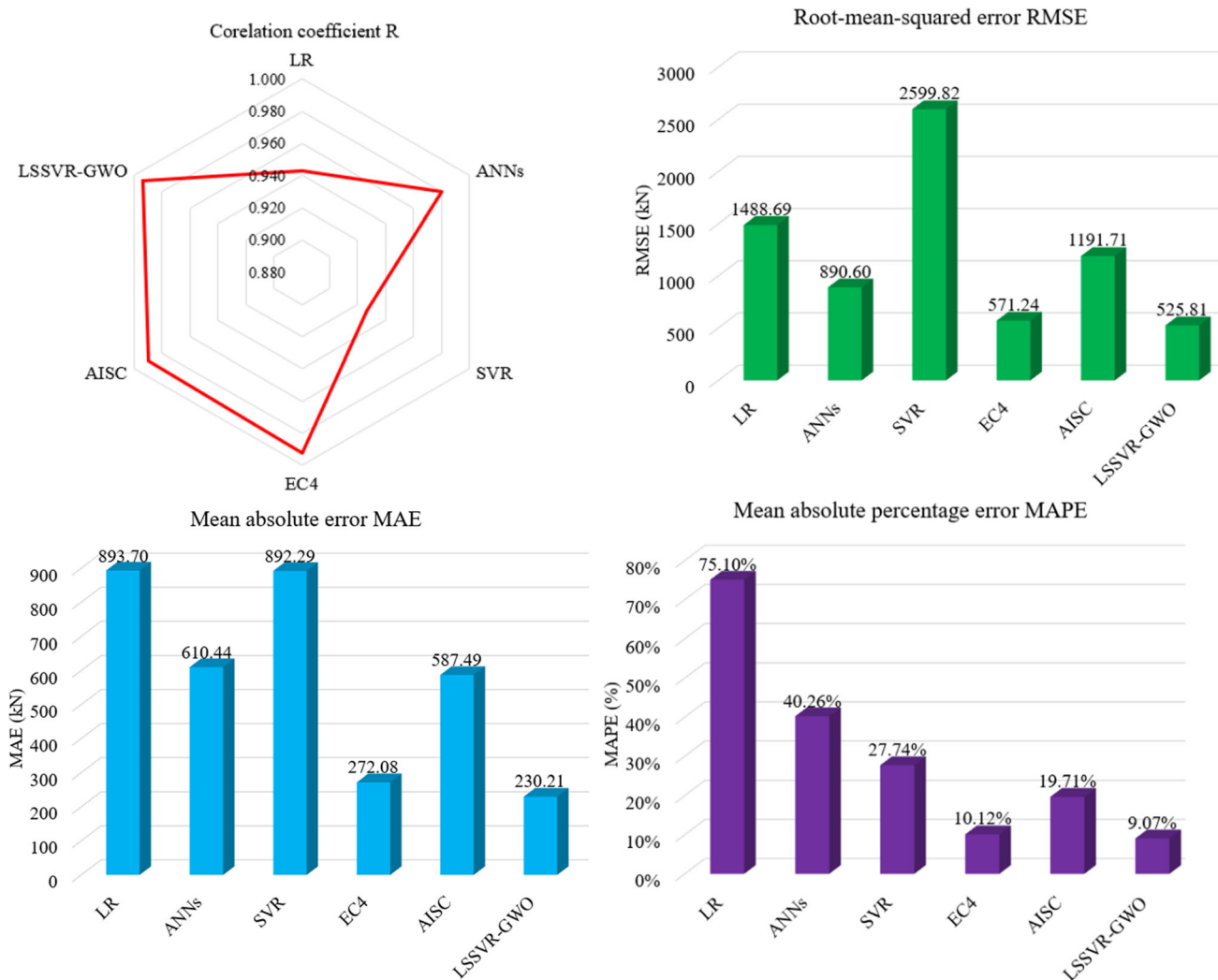


Fig. 12 Performance comparisons among the proposed model and other models

Their predictive performance was relatively better than the LR model. Their average MAPE values were 40.26% and 27.74% for the ANNs and SVR models, respectively.

Table 6 presents that the EC4 and AISC 2005 were quite effective in calculating the UBC of the CFST columns. Particularly, the EC4 achieved a competitive accuracy in which the R was 0.992, RMSE was 571.24 kN, MAE was 272.08 kN, and MAPE was 10.12%. The AISC performance was less effective than the EC4 code in prediction in terms of statistical indices in Table 6. Figure 11 visualizes the scatter plots of the measured and predicted UBC of CFST columns by the EC4 and AISC codes. The red circles represent for prediction by the AISC code, while the black circles represent for prediction by the EC4.

The average accuracy for prediction in Table 6 shows that the proposed AI model was more effective than the compared models and methods in the UBC prediction of CFST columns. Figure 12 visualizes accuracy comparisons

among the models and methods. The SVR-GWO yielded the lowest errors compared to the other investigated models in which the R was 0.994, RMSE was 525.81 kW, MAE was 230.21 kN, and MAPE was 9.07%. The accuracy improvements by the proposed model were ranged from 10.3 to 87.9% in the MAPE and from 15.4 to 74.2% in the MAE compared to other models and methods. The results confirmed the effectiveness of the proposed SVR-GWO, and it was suggested as an AI-based alternative tool for calculating the UBC of CFST columns in structural design.

5 Conclusions

This study proposed an AI-based method for predicting the UBC of CFST columns in structural design. The proposed model combined the SVR as a prediction engine and the GWO as a metaheuristic optimization algorithm. The SVR-

GWO model considers the influencing factors such as the column diameter (D), thickness of steel tube (t), yield stress of steel (f_y), compressive strength of concrete (f_c), column length (L), D/t ratio (D/t) as model inputs for predicting the UBC of CFST columns.

A large dataset was collected in this study to evaluate the proposed SVR-GWO model that consists of 802 samples of experimental tests circular CFST short columns. The used concretes in the experiments consist of the NSC (49%), HSC (23%), and UHSC (28%). The average UBC N_u of CFST columns in the dataset was 3095.70 kN with a standard deviation of 4476.56 kN that reveals the wide range of N_u . The evaluation process has the learning phase and the test phase in which the dataset was split randomly to the learning dataset and the test dataset. The learning dataset was to train and optimize the AI models, which accounts for 90% of the sample size of the original dataset. Meanwhile, the test dataset aimed to test the performance of the trained and optimized AI models for predicting the UBC of circular CFST short columns.

The AI models were evaluated 10 times using a k -fold cross-validation method to ensure the generalizability in the model evaluation. The evaluation results by a large dataset of experimental tests of 802 samples revealed that the SVR-GWO model yielded the outstanding performance in which the R was 0.994, RMSE was 525.81 kW, MAE was 230.21 kN, and MAPE was 9.07%. In comparison with other baseline AI models (i.e., LR, ANNs, SVR) and empirical methods (i.e., EC4 and AISC), the accuracy improvements by the proposed model were ranged from 10.3 to 87.9% in the MAPE and from 15.4 to 74.2% in the MAE.

As contributions of this study, the results confirmed the effectiveness of the proposed model and it was suggested as an AI-based alternative tool for determining the UBC of CFST columns in structural design in practice. In the proposed model, the GWO was used to fine-tune hyperparameters of the SVR model which can improve predictive performance compared to baseline models. This study contributes to promote the application of AI techniques in the structural design domain.

Acknowledgements This research is funded by Vietnam Ministry of Education and Training under the Project Code B2020-DNA-04.

Compliance with ethical standards

Conflict of interest The authors declare that they have no conflict of interest.

References

- Han L-H, Li W, Bjorhovde R (2014) Developments and advanced applications of concrete-filled steel tubular (CFST) structures: members. *J Constr Steel Res* 100:211–228
- Giakoumelis G, Lam D (2004) Axial capacity of circular concrete-filled tube columns. *J Constr Steel Res* 60:1049–1068
- Le Hoang A, Fehling E (2017) Influence of steel fiber content and aspect ratio on the uniaxial tensile and compressive behavior of ultra high performance concrete. *Constr Build Mater* 153:790–806. <https://doi.org/10.1016/j.conbuildmat.2017.07.130>
- De Nardin S, Debs A (2007) Axial load behaviour of concrete-filled steel tubular columns. *Proc Inst Civ Eng-Struct Build* 160:13–22
- De Oliveira WLADN, De Cresce El Debs ALH, El Debs MK (2010) Evaluation of passive confinement in CFT columns. *J Constr Steel Res* 66(4):487–495
- Gardner NJ, Jacobson ER (1967) Structural behavior of concrete-filled steel tubes. *ACI Struct J* 64(7):404–412
- Goode CD (2008) Composite columns—1819 tests on concrete-filled steel tube columns compared with Eurocode 4. 86:33–38
- Guler SAM, Copur A (2013) Axial capacity and ductility of circular UHPC-filled steel tube columns. *Mag Concr Res* 65(15):898–905
- Liew JYR, Xiong MX, Xiong D (2016) Design of concrete filled tubular beam-columns with high strength steel and concrete. *Structures*. <https://doi.org/10.1016/j.istruc.2016.05.005>
- An H, Le FE, Thai Duc-Kien, Nguyen Chau V (2018) Simplified stress-strain model for circular steel tube confined UHPC and UHPFRC columns. *Steel Compos Struct* 29(1):125–138
- Das S, Dey A, Pal A, Roy N (2015) Applications of artificial intelligence in machine learning: review and prospect. *Int J Comput Appl* 115:31–41. <https://doi.org/10.5120/20182-2402>
- Juez-Gil M, Erdakov IN, Bustillo A, Pimenov DY (2019) A regression-tree multilayer-perceptron hybrid strategy for the prediction of ore crushing-plate lifetimes. *J Adv Res* 18:173–184. <https://doi.org/10.1016/j.jare.2019.03.008>
- Mikolajczyk T, Nowicki K, Kłodowski A, Pimenov DY (2017) Neural network approach for automatic image analysis of cutting edge wear. *Mech Syst Signal Process* 88:100–110. <https://doi.org/10.1016/j.ymsp.2016.11.026>
- Ranjan J, Patra K, Szalay T, Mia M, Gupta M, Song Q, Krolczyk G, Chudy R, Pashnyov V, Pimenov D (2020) Artificial intelligence-based hole quality prediction in micro-drilling using multiple sensors. *Sensors* 20:885. <https://doi.org/10.3390/s20030885>
- Pham A-D, Ngo N-T, Nguyen T-K (2020) Machine learning for predicting long-term deflections in reinforce concrete flexural structures. *J Comput Des Eng*. <https://doi.org/10.1093/jcde/qwaa010>
- Chou J-S, Ngo N-T, Pham A-D (2016) Shear strength prediction in reinforced concrete deep beams using nature-inspired meta-heuristic support vector regression. *J Comput Civ Eng* 30(1):04015002. [https://doi.org/10.1061/\(ASCE\)CP.1943-5487.0000466](https://doi.org/10.1061/(ASCE)CP.1943-5487.0000466)
- Pham A-D, Ngo N-T, Ha Truong TT, Huynh N-T, Truong N-S (2020) Predicting energy consumption in multiple buildings using machine learning for improving energy efficiency and sustainability. *J Clean Prod* 260:121082. <https://doi.org/10.1016/j.jclepro.2020.121082>
- Chou JS, Ngo NT, Chong WK, Gibson GE (2016) 16-Big data analytics and cloud computing for sustainable building energy efficiency. In: Pacheco-Torgal F, Rasmussen E, Granqvist C-G, Ivanov V, Kaklauskas A, Makonin S (eds) *Start-up creation*. Woodhead Publishing, Sawston, pp 397–412. <https://doi.org/10.1016/B978-0-08-100546-0.00016-9>

19. Hsieh Y-A, Tsai YJ (2020) Machine learning for crack detection: review and model performance comparison. *J Comput Civ Eng* 34(5):04020038. [https://doi.org/10.1061/\(ASCE\)CP.1943-5487.0000918](https://doi.org/10.1061/(ASCE)CP.1943-5487.0000918)
20. Chong A, Xu W, Chao S, Ngo N-T (2019) Continuous-time Bayesian calibration of energy models using BIM and energy data. *Energy Build* 194:177–190. <https://doi.org/10.1016/j.enbuild.2019.04.017>
21. Fan Z, Chiong R, Hu Z, Lin Y (2020) A fuzzy weighted relative error support vector machine for reverse prediction of concrete components. *Comput Struct* 230:106171. <https://doi.org/10.1016/j.compstruc.2019.106171>
22. Chou J-S, Ngo N-T (2018) Engineering strength of fiber-reinforced soil estimated by swarm intelligence optimized regression system. *Neural Comput Appl* 30(7):2129–2144. <https://doi.org/10.1007/s00521-016-2739-0>
23. Pham A-D, Ngo N-T, Nguyen Q-T, Truong N-S (2020) Hybrid machine learning for predicting strength of sustainable concrete. *Soft Comput*. <https://doi.org/10.1007/s00500-020-04848-1>
24. Gholampour A, Mansouri I, Kisi O, Ozbakkaloglu T (2020) Evaluation of mechanical properties of concretes containing coarse recycled concrete aggregates using multivariate adaptive regression splines (MARS), M5 model tree (M5Tree), and least squares support vector regression (LSSVR) models. *Neural Comput Appl* 32(1):295–308. <https://doi.org/10.1007/s00521-018-3630-y>
25. Chuang H-C, Chen C-C, Li S-T (2020) Incorporating monotonic domain knowledge in support vector learning for data mining regression problems. *Neural Comput Appl* 32(15):11791–11805. <https://doi.org/10.1007/s00521-019-04661-4>
26. Das S, Choudhury S (2020) Evaluation of effective stiffness of RC column sections by support vector regression approach. *Neural Comput Appl* 32(11):6997–7007. <https://doi.org/10.1007/s00521-019-04190-0>
27. Mirjalili S, Mirjalili SM, Lewis A (2014) Grey wolf optimizer. *Adv Eng Softw* 69:46–61. <https://doi.org/10.1016/j.advengsoft.2013.12.007>
28. Uy B, Khan M, Tao PZ, Mashiri F (2013) Behaviour and design of high strength steel-concrete filled columns. In: Proceedings of the 2013 world congress on advances in structural engineering and mechanics (ASEM13), Jeju, Korea, pp 150–167
29. Johansson M (2002) Composite action and confinement effects in tubular steel-concrete columns. *Doktorsavhandlingar vid Chalmers Tekniska Hogskola I + 1-77*
30. Tue NVS, Simsch G, Schmidt D (2004) Bearing capacity of stub columns made of NSC, HSC and UHPC confined by a steel tube. *Proc of 1st Int Symposium on Ultra High Performance Concrete*. Kassel, Germany, March, pp 339–350
31. Ahmadi M, Naderpour H, Kheyroddin A (2017) ANN Model for Predicting the Compressive Strength of Circular Steel-Confined Concrete. *International Journal of Civil Engineering* 15:213–221. <https://doi.org/10.1007/s40999-016-0096-0>
32. Jegadesh J, Jayalekshmi S (2015) Application of artificial neural network for calculation of axial capacity of circular concrete filled steel Tubular Columns. *Int J Earth Sci Eng* 8
33. Du Y, Chen Z, Zhang C, Cao X (2017) Research on axial bearing capacity of rectangular concrete-filled steel tubular columns based on artificial neural networks. *Front Comput Sci* 11:1–11. <https://doi.org/10.1007/s11704-016-5113-6>
34. Tran V-L, Thai D-K, Kim S-E (2019) Application of ANN in predicting ACC of SCFST column. *Compos Struct*. <https://doi.org/10.1016/j.compstruct.2019.111332>
35. Rizzo F, Caracoglia L (2020) Artificial Neural Network model to predict the flutter velocity of suspension bridges. *Comput Struct* 233:106236. <https://doi.org/10.1016/j.compstruc.2020.106236>
36. Sarir P, Chen J, Asteris P, Jahed Armaghani D, Tahir M (2019) Developing GEP tree-based, neuro-swarm, and whale optimization models for evaluation of bearing capacity of concrete-filled steel tube columns. *Eng Comput*. <https://doi.org/10.1007/s00366-019-00808-y>
37. Avci-Karatas C (2019) Prediction of ultimate load capacity of concrete-filled steel tube columns using multivariate adaptive regression splines (MARS). *Steel and Composite Structures* 33(4):583–594. <https://doi.org/10.12989/scs.2019.33.4.583>
38. Nour AI, Güneysi EM (2019) Prediction model on compressive strength of recycled aggregate concrete filled steel tube columns. *Compos B Eng* 173:106938. <https://doi.org/10.1016/j.compositesb.2019.106938>
39. Ahmadi M, Naderpour H, Kheyroddin A (2014) Utilization of artificial neural networks to prediction of the capacity of CCFT short columns subject to short term axial load. *Arch Civ Mech Eng*. <https://doi.org/10.1016/j.acme.2014.01.006>
40. Liu J (2013) Neural networks method applied to the property study of steel-concrete composite columns under axial compression. *Int J Smart Sens Intell Syst* 6:548–567. <https://doi.org/10.21307/ijssis-2017-554>
41. Mete Güneysi E, Gültekin A, Mermerdaş K (2016) Ultimate capacity prediction of axially loaded CFST short columns. *Int J Steel Struct* 16:99–114. <https://doi.org/10.1007/s13296-016-3009-9>
42. Institution BS (2004) Design of Composite Steel and Concrete Structures, Part 1.1, General Rules and Rules for Building. BS EN 1994-1-1. British Standards Institution, London, UK
43. 360-10) AIOSCAA (2010) Specification for structural steel buildings. An American National Standard, U.S
44. Suykens JAK, Gestel TV, Brabanter JD, Moor BD, Vandewalle J (2002) Least squares support vector machines. World Scientific, Singapore
45. ASCCS AoS-CCS (2019) ASCCS composite columns database. University of Bradford. <https://www.bradford.ac.uk/sustainable-environments/asccs/columns-database/>. Accessed October 30 2019
46. Wu X, Kumar V, Quinlan JR, Ghosh J, Yang Q, Motoda H, McLachlan GJ, Ng A, Liu B, Yu PS, Zhou Z-H, Steinbach M, Hand DJ, Steinberg D (2007) Top 10 algorithms in data mining. *Knowl Inf Syst* 14(1):1–37. <https://doi.org/10.1007/s10115-007-0114-2>
47. Vapnik VN (1995) The nature of statistical learning theory. Springer, New York
48. Abd AM, Abd SM (2017) Modelling the strength of lightweight foamed concrete using support vector machine (SVM). *Case Stud Constr Mater* 6:8–15. <https://doi.org/10.1016/j.cscm.2016.11.002>
49. Haykin S (1998) Neural networks: a comprehensive foundation. Prentice Hall PTR, Upper Saddle River
50. Neter J, Kutner MH, Nachtsheim CJ, Wasserman W (1996) Applied linear statistical models, 4th edn. McGraw-Hill, Irwin
51. Waikato Uo (2020) Weka 3—Data Mining with Open Source Machine Learning University of Waikato. <https://www.cs.waikato.ac.nz/ml/weka/>

Publisher's Note Springer Nature remains neutral with regard to jurisdictional claims in published maps and institutional affiliations.